Anal. Bioanal. Electrochem., Vol. 14, No. 3, 2022, 270-289

Analytical & Bioanalytical Electrochemistry

www.abechem.com

Full Paper

Two-Step Protein-Film Voltammetry Associated with Intermediate Reversible Chemical Reaction-Diagnostic Criteria for Characterizing Systems with Inverted Potentials in Square-Wave Voltammetry

Pavlinka Kokoskarova, and Rubin Gulaboski*

Faculty of Medical Sciences, Goce Delcev University Stip, Republic of Macedonia

*Corresponding Author, Tel.: +38975331078

E-Mail: rubin.gulaboski@ugd.edu.mk

Received: 13 February 2022 / Received in revised form: 24 March 2022

Accepted: 24 March 2022 / Published online: 31 March 2022

Abstract- Many electron transfer mechanisms of important physiological systems commonly occur as multistep electrode reactions that are initiated by a gain or loss of an electron. The product of initial electrochemical reaction might subsequently participate in chemical and/or electrochemical reaction(s), in which the final product of entire mechanism is generated. Therefore, a proper understanding of electron transfer phenomena is of outmost importance to get information about mechanism going on in the redox transformation of relevant physiological systems. In this work, we focus on theoretical voltammetric features of complex multielectron surface electrode mechanisms, in which two electron transfer steps are bridged by a reversible chemical reaction. Special attention is paid to systems with so-called "inverted potentials", in which the second electron transfer requires less energy to occur than the first one. Square-wave voltammetry (SWV) of so-called "surface ECrevE mechanism" is explored as a valuable technique that can give relevant information about diagnostics of this mechanism. The presented model is suitable to study the activity of various enzymes and lipophilic organic compounds by exploring the "protein-film voltammetry" scenario.

Keywords- Protein-film voltammetry; Two-step mechanisms; Surface $EC_{rev}E$ mechanism; Kinetics of chemical reactions; Systems with inverted redox potentials

1. INTRODUCTION

Many important physiological systems exhibit their activity via a complex redox process that occurs in a two-step electron transfer, with electrons being exchanged in a consecutive

manner [1-3]. In majority of the two-step electrode mechanisms, both electron transfers are commonly bridged by a chemical reaction [2-5]. "ECE mechanism" is a common electrochemical designation of such a multielectron sequential redox transformation. Physiological multielectron redox compounds in which protonation/deprotonation reaction bridges the product of the first and the reactant of the second electron transfer step are probably the most important systems belonging to this mechanism. Coenzyme Q members [2,4], flavins [2], polyphenols [2,4], cytochromes, and metalloproteins [2,5] are just some of the representative examples whose redox transformation can be described by the ECE mechanism. In order to get relevant information from the multielectron redox transformation mechanism, it is important to explore a methodology to recognize the nature of electrode mechanism going on. That will reveal significant aspects about the stability and reactivity of different oxidation states of studied systems. As cyclic voltammetry [6], and square-wave voltammetry [7] are mainly explored to study theoretically the ECE mechanisms [8-10], in most of the studies presented in the literature, a two-step surface mechanism associated with an irreversible chemical reaction ($EC_{irr}E$ mechanism) is mainly considered. In this work, we elaborate a two-step surface electrode mechanism, with a thermodynamically reversible chemical reaction bridging the two electron transfer steps. The new insights on the electrochemical features of so-called "surface $EC_{rev}E$ mechanism" are considered under conditions of protein-film square-wave voltammetry. We elaborate an initial scenario in which both peaks are separated of -150 mV or more (i.e. the difference in formal potentials between the second and the first SW peak). However, scenario of so-called "inverted potentials", in which the energy of the second electron transfer is lower than that of the first electron transfer step, is also analyzed. Redox systems with inverted potentials will produce single patterns in SWV, with features of the voltammograms hiding the kinetics of both electron transfer steps, and the kinetics and thermodynamics of chemical reaction, as well. In the last scenario, it is a challenging task to recognize whether the only SWV peak that will appear is a consequence of two consecutive electron transfers, or it is due to the occurrence of a single 2-electron transfer. We also focus on developing an approach in SWV to recognize a particular two-step consecutive electrode mechanism in case of "inverted potentials" of both electron transfer steps. The mechanism considered in this work is particularly suitable to get insight into the redox behaviour of many lipophilic enzymes [5,11-14], and other physiologically relevant compounds that contain quinine/hydroquinone moiety or disulfide -S-S- bonds as redox active centers in their structures [2,4,5].

2. MATHEMATICAL MODEL AND PARAMETERS AFFECTING THE FEATURES OF SIMULATED SW VOLTAMMETRIC PATTERNS

In the mathematical model considered we elaborate a two-step consecutive electrode transformation of initial redox-active adsorbate (Ox), whose molecules are firmly adsorbed on

the working electrode surface. In addition, we assume that both electron transfer steps are bridged with a reversible ("rev") chemical step. The abbreviation of this model is "surface $EC_{rev}E$ mechanism", and it can be described by the following reaction scheme:

$$\mathrm{Ox(ads) + n_1e^-} \overset{k_{s,1}^{e}}{\rightleftharpoons} \mathrm{Int_1(ads) + Y} \underset{k_b}{\overset{k_f}{\rightleftharpoons}} \mathrm{Int_2(ads) + n_2e^-} \overset{k_{s,2}^{e}}{\rightleftharpoons} \mathrm{Red(ads)} \qquad \text{(I)}$$

At the beginning of the experiment, we assume that only Ox(ads) and "Y" species are present in the electrochemical cell, and they do not react between them. With "Int_1(ads)" we assign intermediate species created upon reduction of Ox(ads) in the first electron transfer step. By "Y" we define an electrochemically non-active substrate (in the region of applied bias). "Y" can react reversibly and selectively with "Int_1(ads)" species only, while creating "Int_2(ads)" redox species. We suppose that no electrochemical reaction of any kind takes place from the dissolved state. "Red(ads)" species are the ultimate redox-active species, generated electrochemically in the course of the second electron transfer step via reduction from "Int_2(ads)". We assume that "Y" substrate is present in large excess in the electrochemical cell, and it shows no electrochemical activity at the working electrode in the frame of applied potentials. Therefore, the concentration of "Y" remains constant at the electrode surface in the course of the voltammetric experiment. Consequently, we assume that the chemical step in mechanism (1) is of pseudo-first order. Elaborated $EC_{rev}E$ mechanism is solved under the following conditions:

$t = 0$; $\Gamma(\mathrm{Ox}) = \Gamma^*(\mathrm{Ox})$; $\Gamma(\mathrm{Int_1}) = \Gamma(\mathrm{Int_2}) = \Gamma(\mathrm{Red}) = 0$ (1)

$t > 0$; $\Gamma(\mathrm{Ox}) + \Gamma(\mathrm{Int_1}) + \Gamma(\mathrm{Int_2}) + \Gamma(\mathrm{Red}) = \Gamma^*(\mathrm{Ox})$ (2)

For $t > 0$, the following conditions apply:

$$\mathrm{d}\Gamma(\mathrm{Ox})/\mathrm{d}t = -I_1/(n_1FS) \qquad (3)$$

$$\mathrm{d}\Gamma(\mathrm{Int_1})/\mathrm{d}t = I_1/(n_1FS) - k_f\Gamma(\mathrm{Int_1}) + k_b\Gamma(\mathrm{Int_2}) \qquad (4)$$

$$\mathrm{d}\Gamma(\mathrm{Int_2})/\mathrm{d}t = I_2/(n_2FS) + k_f\Gamma(\mathrm{Int_1}) - k_b\Gamma(\mathrm{Int_2}) \qquad (5)$$

$$\mathrm{d}\Gamma(\mathrm{Red})/\mathrm{d}t = I_2/(n_2FS) \qquad (6)$$

We consider a Butler-Volmer formalism holding for the interdependence between the potential applied, electric current, the surface concentrations (Γ) of all species involved, and the electrode reaction parameters that affect the features of theoretical voltammograms of considered mechanism (equations 7 and 8).

$$(I_1/n_1FS) = k_{s.1}^{e}\exp(-\alpha_1\Phi_1)\,[\Gamma(\mathrm{Ox}) - \exp(\Phi_1)\,\Gamma(\mathrm{Int_1})] \qquad (7)$$

$$(I_2/n_2FS) = k_{s.2}^{e}\exp(-\alpha_2\Phi_2)\,[\Gamma(\mathrm{Int_2}) - \exp(\Phi_2)\,\Gamma(\mathrm{Red})] \qquad (8)$$

Solutions to integral equations of this mathematical model have been obtained by means of a numerical integration method that is presented in more detail elsewhere [7]. For the numerical solution of the elaborated model, the time increment of each potential SW pulse (d) was defined as $d = 1/(50f)$. In the last equation, f is the frequency of the potential modulation in SWV. It

means that each SW half-period $\tau/2$ was divided into 25-time increments. In the Supplementary material in this work, we give a detailed MATHCAD file containing all recurrent formulas, the form of the potential signal, and all other parameters needed for calculating theoretical voltammograms of the considered surface $EC_{rev}E$ mechanism. In the theoretical model, we define the reduction currents to have a positive sign, while a negative sign is ascribed to oxidation currents. All potentials are defined *vs*. the standard redox potential of the first electrode process that happens at more positive potentials (peak I). In all simulations, the starting potential is set to a positive value, and it runs toward a final more negative bias.

The overall normalized dimensionless current Ψ of calculated SW patterns is defined as a sum of the currents associated to the first and the second electrode step, i.e. $\Psi = \Psi_I + \Psi_{II}$. The dimensionless currents related to each of both electrode steps are defined as $\Psi_I = I_1/[(n_1FSf\Gamma^*(Ox))]$ and $\Psi_{II} = I_2/[(n_2FSf\Gamma^*(Ox))]$. I stays for the magnitude of the electric current, while n_1 and n_2 are the numbers of electrons exchanged in the first and the second electron transfer step, respectively. In all calculations, we set an approximation that $n_1 = n_2 = n = 1$. With S we assign the active surface area of the working electrode, while f is the SW frequency defined as $f = 1/(2t_p)$. In the last equation, time parameter t_p is a duration of a single potential pulse in SWV. With "Γ" we define the surface concentration, while $\Gamma^*(Ox)$ stays for the total surface concentration. This, in fact, is the initial surface concentration of adsorbed Ox species. Φ is the symbol of a dimensionless potential defined as $\Phi_1 = nF(E - E_1^{\theta'}/RT)$ *and* $\Phi_2 = nF(E - E_2^{\theta'}/RT)$, where $E_1^{\theta'}$ and $E_2^{\theta'}$ are the formal redox potentials of first and second electrode step, respectively. α stays for the electron transfer coefficient, which is assumed to be $\alpha = 0.5$ for both electrode transfer steps. T is a symbol for the thermodynamic temperature (T was set to 298 K in all calculations), R is the universal gas constant, and F is the Faraday constant. In addition, calculated SW voltammograms in all considered mechanisms are affected by several dimensionless parameters. The dimensionless electrode kinetic parameters $K\mathrm{I} = k_{s,1}^{\theta}/f$ and $K\mathrm{II} = k_{s,2}^{\theta}/f$ are linked to the kinetics of electron transfer reactions between the working electrode and the redox analytes of corresponding electron transfers steps. Moreover, the features of calculated voltammograms are affected by a dimensionless chemical parameter K_{chem} that is defined as $K_{chem} = \varepsilon/f$. In last equation, $\varepsilon = (k_f + k_b)$ is a chemical parameter that is defined as a sum of the first order rate constants k_f and k_b of forward and backward chemical reaction, respectively. At this stage, it is worth to note that the chemical parameter K_{chem} is of pseudo-first order, since it depends on the concentration of "Y" substrate $c(Y)$ in the following manner: $K_{chem} = [k_f^{\theta'}c(Y) + k_b]/f$, where $k_f^{\theta'}$ is the real rate constant of the forward chemical step. Additionally, the major attributes of theoretical SW voltammograms depend on the equilibrium constant K_{eq} defined as $K_{eq} = k_f/k_b$.

In all calculations, the major parameters of applied bias were set to: SW frequency $f = 10$ Hz, SW amplitude $E_{sw} = 50$ mV, and potential step $dE = 4$ mV. More details of the algorithm used can be found in the Supplementary file of this work, in which we give all recurrent

formulas to calculate SW voltammograms. By exploring the working file given in the Supplementary, one can simulate plethora of scenarios in respect to the kinetics and thermodynamics of both electron transfer steps, while also considering various kinetics and thermodynamics of the chemical step. We used commercially available MATHCAD 14 software for calculating the SW voltammograms. The net current in all simulated voltammetric patterns is represented by black colour, while the forward (reduction) currents are assigned with blue colour. Red colour is associated with the backward (reoxidation) current branches at all simulated voltammograms.

3. RESULTS AND DISCUSSION

Before we start elaborating on the results of a surface $EC_{rev}E$ mechanism in SWV, it is worth to mention several general aspects about the effect of coupled chemical reaction to the features of electron transfer steps. Under the term "coupling" one considers a chemical reaction that might affect the thermodynamics of the electron transfer step going on between the working electrode and a defined redox adsorbate. Protonation/deprotonation is one type of chemical reaction that is commonly associated with electron transfer steps of many physiological systems [1-5]. While the chemical reactions featuring fast kinetics might affect the thermodynamics of the electrode step by displacing the equilibrium of redox adsorbates, slow chemical reactions commonly influence the kinetics of the overall reaction mechanism. As we noted in the previous section, the dimensionless chemical rate parameters of electron transfer steps are both affected by the SW frequency. Moreover, the SW frequency influences the rate of the chemical reaction (via K_{chem}), too. In order to avoid misinterpretations of the results obtained by varying the SW frequency [15], in all simulations performed, the rate of the chemical reaction was altered via modifying the concentration of "electrochemically inactive" substrate c(Y) at constant frequency.

When simulating various scenarios of this complex mechanism, it was found that a magnitude of potential separation between peak II and peak I (i.e. $E^{\ominus}_2$-$E^{\ominus}_1$) more negative than -150 mV leads to voltammetric patterns whose characteristics can be described by the features of surface EC_{rev} mechanism for peak I, and with the surface $C_{rev}E$ mechanism for peak II. Since a comprehensive elaboration of SWV features of surface EC_{rev} mechanism and surface $C_{rev}E$ mechanism is given in [16,17] and [17,18], respectively, we advise the readers for more information to these works. In [16,18], one also finds relevant methodologies applicable for the determination of all pertinent kinetic and thermodynamic parameters of each step involved in the surface $EC_{rev}E$ mechanism. In the first part of this section, we explain the most relevant results of both separated peaks of a surface $EC_{rev}E$ mechanism, which can be useful for experimentalists.

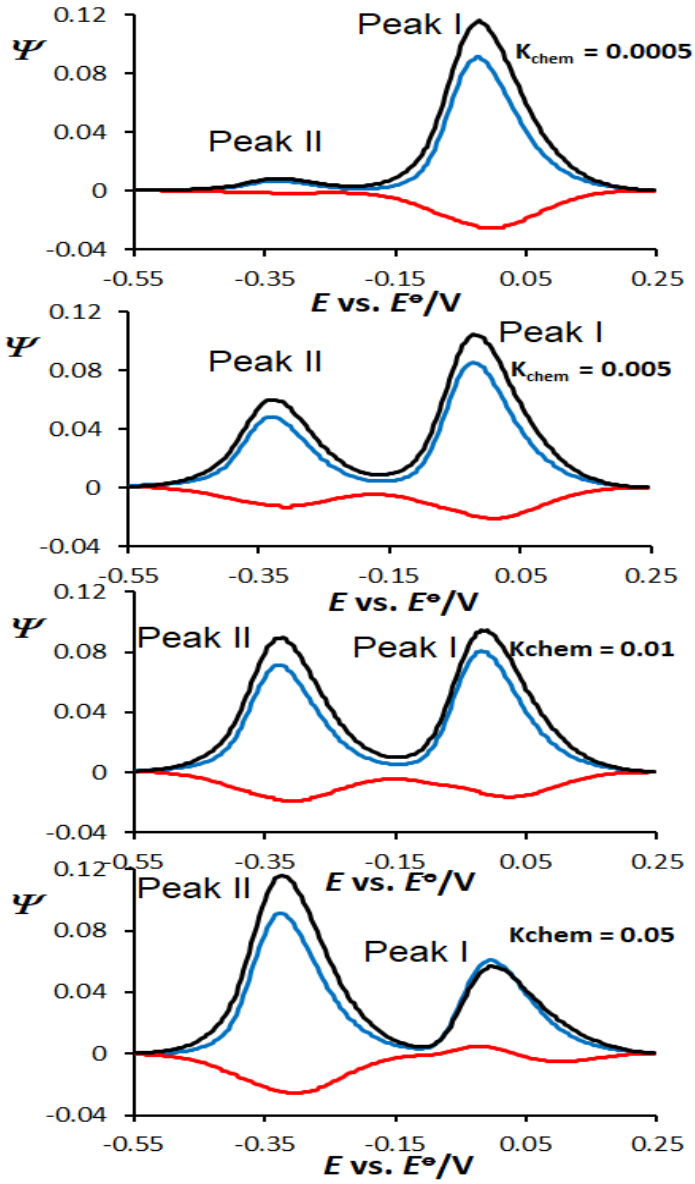

Figure 1. Theoretical square-wave voltammograms of a surface EC$_{rev}$E mechanism representing the effect of the chemical rate parameter K_{chem}. Voltammograms are simulated at the potential separation of -300 mV between the second and the first electron transfer step. The magnitudes of both *K*I and *K*II were set to 0.05. The magnitude of equilibrium constant was set to K_{eq} = 1000. Magnitudes of K_{chem} used in simulations are given in the charts. Other simulation parameters were as follows: SW frequency f = 10 Hz, SW amplitude E_{sw} = 50 mV, potential step dE = 4 mV, temperature T = 298 K. In all simulations, the electron transfer coefficients of the first and second electrode reaction were set to α = 0.5, while the number of electrons exchanged between the working electrode and the redox adsorbates were $n_1 = n_2 = 1$. All potentials are referred *vs* the standard redox potentials of the first electron transfer step. The net current in all simulated voltammetric patterns is represented by black colour, while the forward (reduction) currents are assigned with blue colour. Red colour is associated with the backward (reoxidation) current branches at all simulated voltammograms

For the case of slow and moderate electron transfer of both SW peaks, the equilibrium constant of chemical reaction affects all features of both SWV peaks of this complex mechanism. For given magnitude of chemical rate parameter K_{chem}, the dependence of $\Psi_{net,p1}$ *vs* log(K_{eq}) of SW peak I has a sigmoidal shape [16] (not shown). The working curves of $\Psi_{net,p1}$ *vs* log(K_{eq}) feature a linear part roughly in the regions -2.5 < log(K_{eq}) < 0.5. In the regions of -2 < log(K_{eq}) < 1, the net SW peak potentials of peak I ($E_{net,p1}$) shift towards more negative potential by increasing K_{eq} [16,17]. For the second SW peak (peak II at Figure 1) that has characteristics of a surface $C_{rev}E$ mechanism, one again observes sigmoidal curves of $\Psi_{net,p2}$ *vs* log(K_{eq}) dependence, with current rising in -2.5 < log(K_{eq}) < 0.5 by increasing the magnitude of K_{eq}. Sigmoidal-like features of the curves of dependence between $E_{net,p2}$ *vs* log(K_{eq}) also exist for peak II, but with position of net SW peak potentials ($E_{net,p2}$) shifting towards more positive potentials by an increase of K_{eq} [18].

What is worth to be emphasized in the scenario of potential separation of -150 mV or more between peak II and peak I, is the effect of the dimensionless chemical rate parameter (K_{chem}) to the features of both SW peaks. Shown in Figure 1 are SW voltammograms simulated for large magnitude of the equilibrium constant of chemical step (K_{eq} = 1000), and for several values of $K_{chem.}$ As expected, an increase of the rate of chemical reaction (portrayed via the magnitude of K_{chem}) leads to a decrease of all current components of peak I, and a concomitant increase of all current components of SWV peak II (Figure 1). For the SW peak II, the working curves of the dependence $\Psi_{net,p2}$ *vs* log(K_{chem}), simulated at several magnitudes of K_{eq}, show sigmoidal features (Figure 2A), with net SWV peak currents increasing in the so-called chemical kinetic region (roughly in the region -2 < log(K_{chem}) < 1). The net SW peak potential dependences of $E_{net,p2}$ *vs* log(K_{chem}) also feature sigmoidal shapes, with slope of the linear parts being a function of K_{eq} (Figure 2B).

The slopes of the linear parts of the curves presented in Figure 2B equal to [(2.303*RT*/(*nF*)]log[(K_{eq})/(1+K_{eq})]. Consequently, from the slope of the linear dependence between the net SW peak potentials of peak II as a function of log(K_{chem}) one can evaluate the magnitude of equilibrium constant of chemical step [18]. For the first SWV peak (peak I), a sigmoidal dependence between $E_{net,p1}$ *vs* log(K_{chem}) is also observed, but with SW peak I moving to more positive values by an increase of the rate of chemical reaction (Figure 3). In such scenario, the slopes of the linear parts of $E_{net,p1}$ *vs* log(K_{chem}) dependences presented in Figure 3B read [(-2.303*RT*/(*nF*)]log[(K_{eq})/(1+K_{eq})]. Therefore, an experimentally observed linear dependence between the net SW peak potentials of peak I as a function of log(K_{chem}) can also give access to the magnitude of equilibrium constant of chemical step as elaborated in [7, 16]. For small magnitudes of K_{eq}, the net SW peak currents of peak I also exhibit a sigmoidal dependence as a function of log(K_{chem}) (Figure 3A). However, as the magnitude of K_{eq} is larger than 0.6, a local maximum appears in the regions -2.5 < log(K_{chem}) < -1 (curve with yellow dots in Figure 3A). This feature of a surface EC mechanism is extensively elaborated in [16, 19],

and it is demonstrated that it is a consequence of the mutual interplay between the rate of electron transfer step, the rate of the chemical step, and the simultaneous occurrence of both steps in the so-called "dead-time" of SW potential pulses [19].

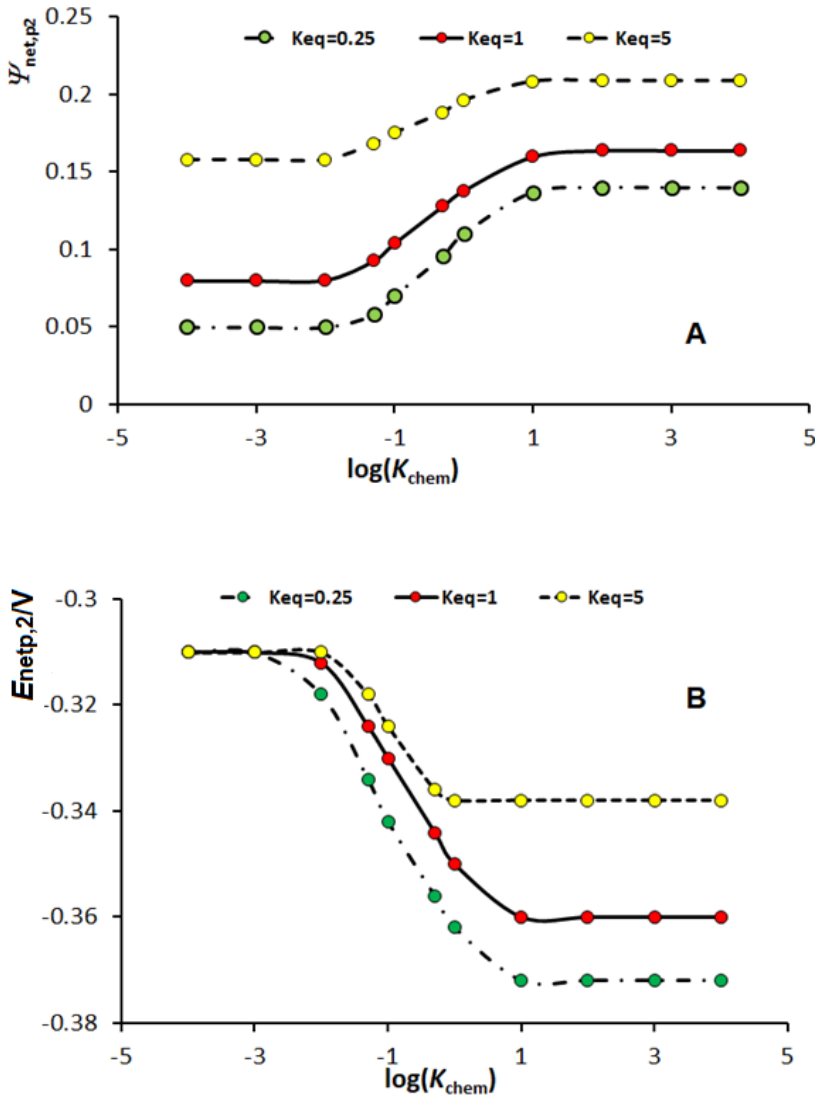

Figure 2. Working curves of the dependences of the net SW peak currents (A) and net SW peak potentials (B) of peak II as a function of the logarithm of dimensionless rate parameter of chemical step. Magnitudes of K_{eq} used in simulations are given in the charts. The value of *K*II was set to 0.15 for this set of simulations. Voltammograms are simulated at the potential separation of -300 mV between the second and the first electron transfer step. Other simulation parameters were the same as those in Figure 1.

The interplay of all these effects, together with the specific current sampling procedure in SWV [7], lead (at moderate rates of the chemical step) to an increase of all current components by an increase of chemical rate parameter. This is quite rare phenomenon met only by surface

EC mechanisms [19]. This effect is even more pronounced in the case of a fast electron transfer step associated with the SW peak I. Patterns in Figure 4 portray the effect of K_{chem} to the main attributes of SW voltammograms simulated for large values of *K*I and *K*II, and for large magnitude of K_{eq}. Note that this is a region of fast electron transfer rates, which is followed by splitting of net SW voltammograms [7]. In such scenario, the first voltammetric process (peak I) exhibits interesting phenomena under the influence of K_{chem}.

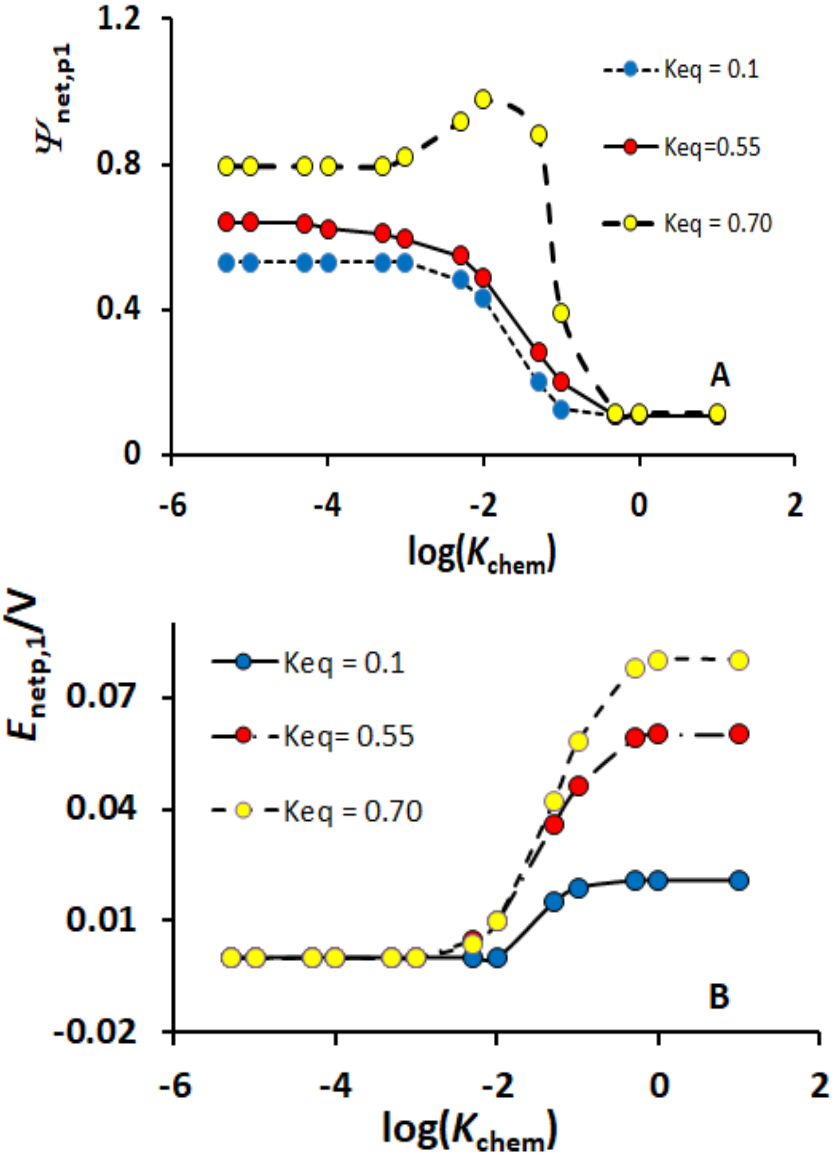

Figure 3. Working curves of the dependences of the net SW peak currents (A) and net SW peak potentials (B) of peak I as a function of the logarithm of dimensionless rate parameter of chemical step. Magnitudes of K_{eq} used in simulations are given in the charts. Voltammograms are simulated at the potential separation of -300 mV between the second and the first electron transfer step. The value of *K*I was set to 0.45 for this set of simulations. Other simulation parameters were the same as those in Figure 1.

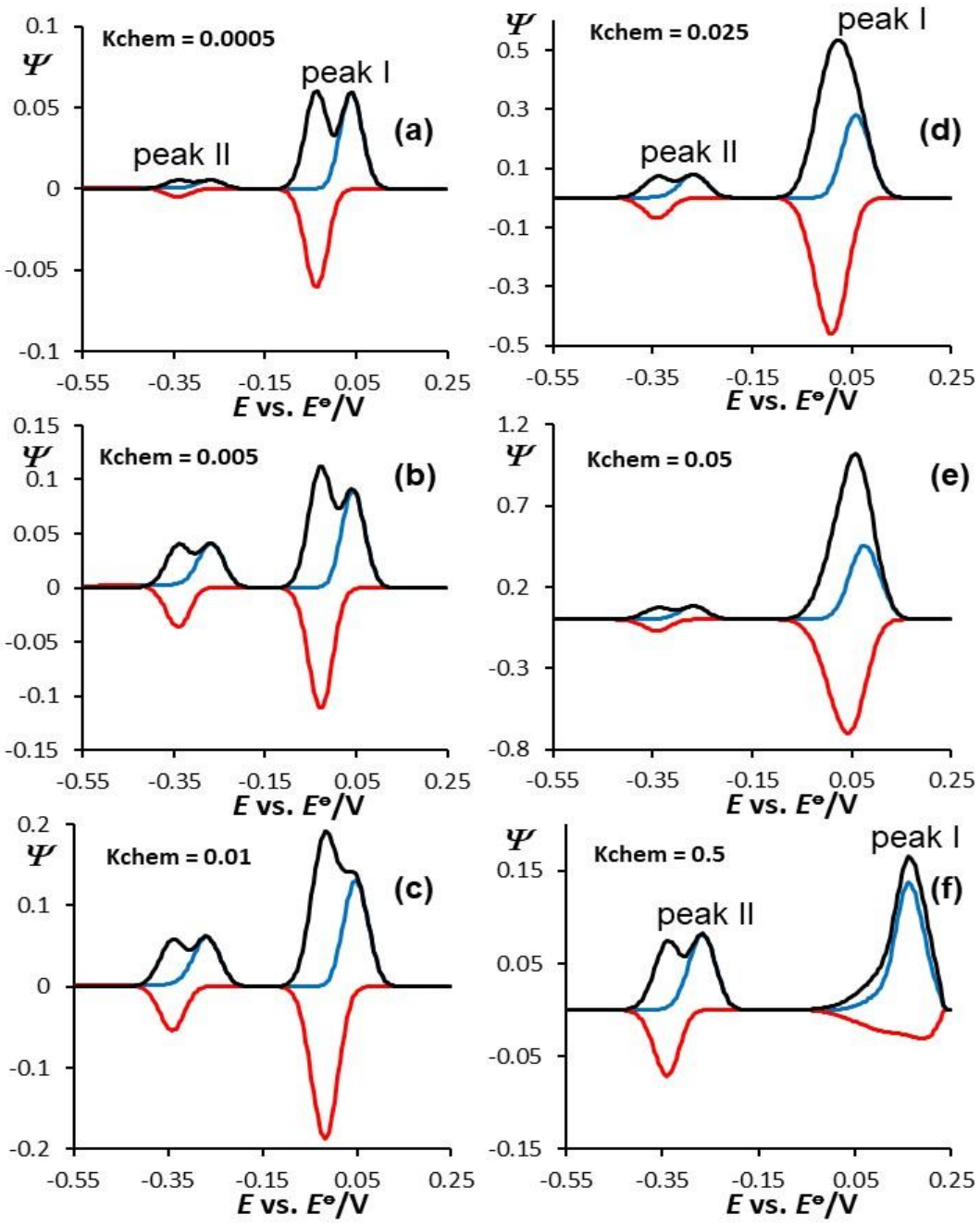

Figure 4. Theoretical square-wave voltammograms of a surface EC$_{rev}$E mechanism portraying the effect of the dimensionless rate parameter of the chemical step K_{chem} in the scenario of fast kinetics of both electron transfer steps. Voltammograms are simulated at the potential separation of -300 mV between peak II and peak I, for K_{eq} = 10000. The values of both *K*I and *K*II were set to 5.0. The magnitudes of K_{chem} used in simulations are given in the charts. Other simulation parameters were the same as those in Figure 1.

Although one expects a current decrease of the first SW peak (peak I) by increasing of the magnitude of the chemical rate parameter K_{chem}, in the region of 0.0005 < K_{chem} < 0.7, however, one observes increasing of all SW current components of peak I (see Figure 4b-d). More

intriguing is the fact that the re-oxidation (backward) current component (which is expected to decrease by increasing of K_{chem}) gains more significantly in its intensity (see Figure 4b-e). Eventually, in the region of large rates of the dimensionless chemical parameter (i.e. for K_{chem} > 0.7, Figure 4f), one observes voltammetric features that are recognized as "common" for the EC_{rev} mechanism [16]. As elaborated in [19], the major causes for the behavior of peak I of the $EC_{rev}E$ mechanism observed in Figure 4b-e are the specific chronoamperometric features of EC_{rev} mechanism in SWV. Moreover, the interplay between the rates of electron transfer and that of the chemical step that take place simultaneously in the so-called "dead time" of SW potential pulses, also contributes to the specific behavior depicted in Figure 4b-e. In [16], we proposed a methodology to explore these specific features as diagnostic criteria to recognize the surface EC_{rev} mechanism characterized with fast electron transfer. In addition, in [16,17] a simple methodology has been developed to evaluate the kinetic parameters relevant to the chemical step from the dependence between the SWV peak currents and the concentration of chemical substrate "Y". At this stage, it is worth to note that for the second electron transfer step (peak II), one can explore the methodology named as "quasireversible maximum" (i.e. the parabolic dependence of the net peak current versus the logarithm of inverse SW frequency) [7] or "split net SW peak" [7] to estimate the standard rate constant of electron transfer $k_{s,1}^{\ominus}$. However, for the first electron transfer step (peak I), one should use some alternative and time-independent methodology as those reported in [20]. This is because the frequency dependence produces complex patterns at surface EC_{rev} mechanism, as comprehensively elaborated in a recent work [15].

In the considered surface $EC_{rev}E$ electrode mechanism, a peculiar situation exists when the energy of second electron transfer is equal or lower than that of the first electron transfer step. Common assignation for this situation is the scenario of "*inverted potentials* of electron transfer steps". In such a sequence of events, both electron transfer steps will be portrayed in a single voltammetric peak in SWV [8]. In experimental electrochemistry, such behaviour is reported in many organic systems that contain conjugated molecules rich with π-electrons. If a consecutive two-step redox transformation occurs in the redox chemistry of such systems, mainly a radical species is formed upon the first reduction step [21]. After the second electron transfer, a stabilization of the formed species (commonly a di-anion) is achieved via charge-delocalization processes. Such a scenario commonly leads to different radii of electrochemically generated species, which will be followed by differences in their solvation energies, too. Structural differences among the species (neutral species, ion radical, or di-ion) also exert an effect on solvation energy. In many systems, such changes in the structure and solvation energies of electrochemically generated species are considered as a major cause of potential inversion phenomenon in their redox chemistry. Organic systems with inverted electrode potentials are found in electrochemistry of nitro derivatives of durene [21], some tetraphenylethylene [21], and anthraquinodimethane derivatives [22], but also in some quinone

derivatives [4,21-23]. In SWV, for given chemical systems, the scenario of both peaks occurring at the same potentials also counts for the situation of positive differences between both peak II and peak I. This is because the occurrence of the first electron transfer process is prerequisite for the second process to take place. Consequently, both processes in SWV will be always portrayed in a single SW peak under such conditions.

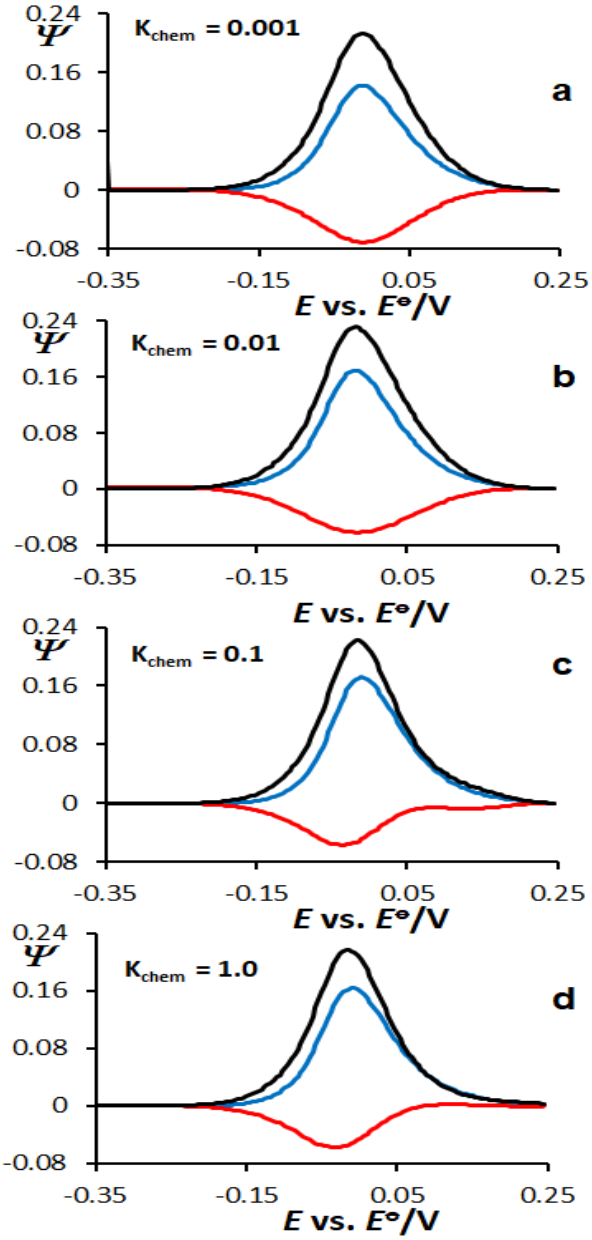

Figure 5. SW voltammograms of a surface EC$_{rev}$E mechanism representing the effect of the dimensionless rate parameter of the chemical step K_{chem} in the scenario of both electron transfer steps taking place at same potential. The magnitude of the chemical equilibrium constant was set to $\boldsymbol{K_{eq}}$ **= 1000**. The values of both *K*I and *K*II were set to 0.1. The magnitudes of K_{chem} used in simulations are given in charts. Other simulation parameters were the same as those in Figure 1.

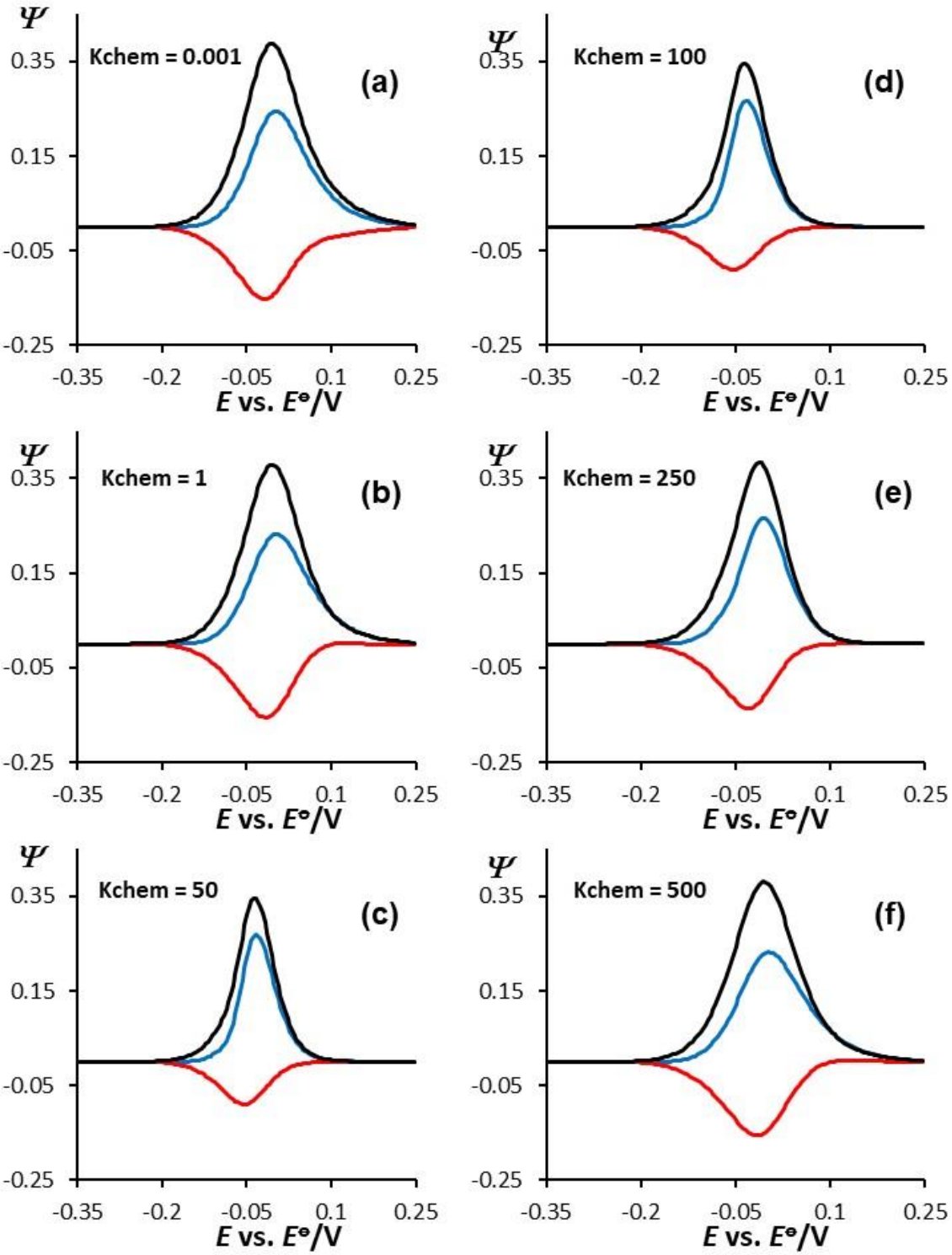

Figure 6. Theoretical SW voltammograms of a surface $EC_{rev}E$ mechanism represent the effect of the dimensionless rate parameter of the chemical step K_{chem} in the scenario of both electron transfer steps taking place at the same potential. The magnitude of the chemical equilibrium constant was set to $\boldsymbol{K_{eq} = 0.05}$. The values of both *K*I and *K*II were set to 0.2. The magnitudes of K_{chem} used in simulations are given in the charts. Other simulation parameters were the same as those in Figure 1.

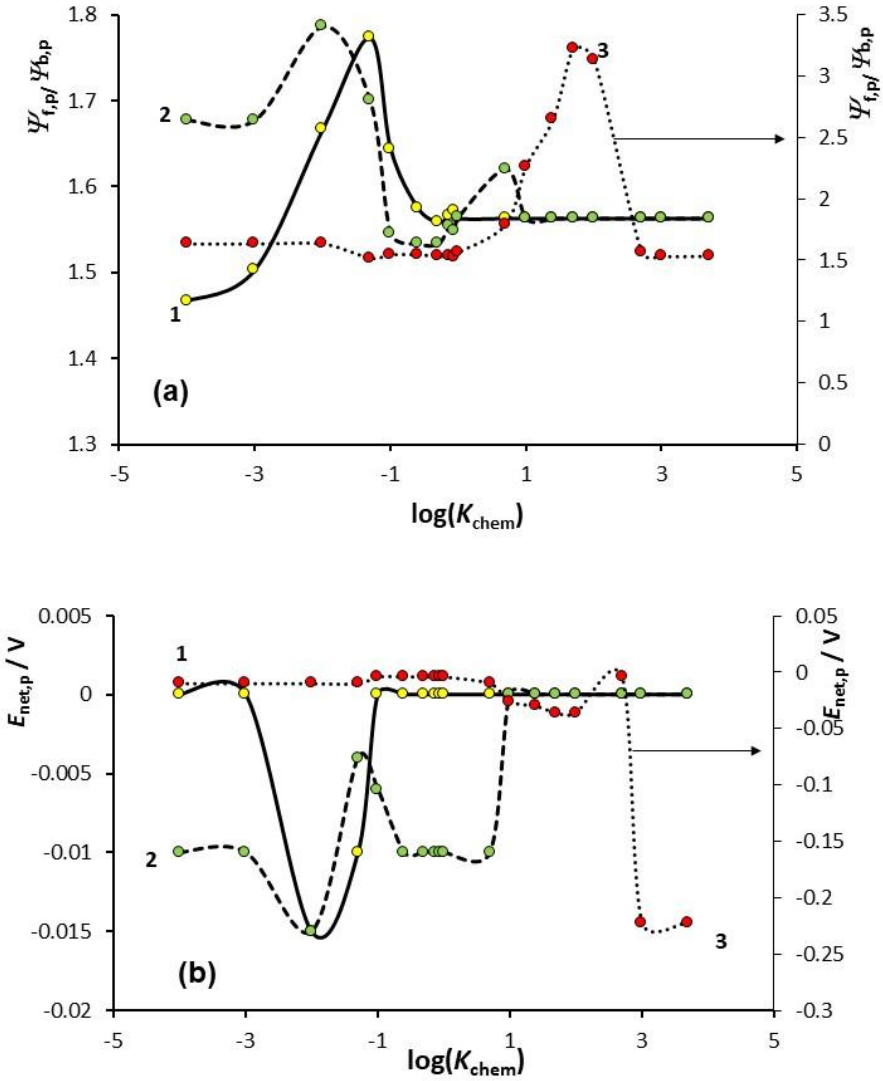

Figure 7. Dependences of the ratio of forward *vs* backward peak currents (a) and net SW peak potentials (b) as a function of log(K_{chem}). Curves are simulated in a scenario of both electron transfer steps happening at the same potential. The magnitudes of the chemical equilibrium constant used in calculations are set to K_{eq} = 100 (1), 1 (2) and 0.05 (3). The values of both *K*I and *K*II were set to 0.2. Other simulation parameters were the same as those in Figure 1.

For experimental systems with inverted potentials, it is of utmost importance to get relevant information on whether their electrochemical transformation occurs in a single 2-electron step, or in two consecutive 1-electron transfer steps, with intermediate species involved between the initial and the final redox species. To achieve this, one should find a relevant methodology to recognize the electrode mechanism of multielectron transfers with inverted potentials. Shown in Figure 5 is a series of SW voltammograms of $EC_{rev}E$ mechanism, calculated by assuming equal kinetics of both electron transfers that take place at a same potential. The voltammograms portray the effect of the dimensionless chemical rate parameter K_{chem} at large values of K_{eq}. Under the conditions defined in Figure 5, one observes minor effects of the rate of chemical

step on the features of the SWV peak, which are slightly more pronounced at larger magnitudes of K_{chem} (Figure 5c-d). At small and moderate values of equilibrium constant of chemical step, one witness much complex effect of chemical rate to the features of SW patterns, for systems with inverted potentials. From the current components of SW voltammograms presented in Figure 6, one witnesses a very complex interplay between the equilibrium constant and the kinetics of the chemical reaction. As in some regions of K_{chem} one recognizes effects similar to surface EC_{rev} mechanism (Figure 6a-c), at larger values of K_{chem} patterns characteristic for $C_{rev}E$ mechanism are observed (Figure 6d-f). As reported in [7,8,16-18], both net SW peak currents and net SW peak potentials of surface EC_{rev} and $C_{rev}E$ mechanism, exhibit a sort of sigmoidal dependences as a function of $\log(K_{chem})$. However, graphs in Figure 7 imply that these functions are quite complex in the case of surface $EC_{rev}E$ mechanism with inverted potentials. Thus, in order to characterize the surface $EC_{rev}E$ mechanism with inverted potentials, one should first develop a relevant methodology to recognize this mechanism in SWV. Shown in Figure 8 is the effect of the dimensionless chemical parameter K_{chem} to the SW voltammograms that are simulated for $K_{eq} = 10$, and $K\mathrm{I} = K\mathrm{II} = 2.0$. As it is elaborated in [16,17], one remarkable feature of a surface EC_{rev} mechanism is the shift of the net SW peak potential towards more positive magnitudes by an increase of K_{chem}. Bearing in mind this fact, it is expected that a successful separation of the overlapped electron transfer steps can be achieved upon the increased rate of the chemical reaction. As presented in Figure 8, by an increase of the chemical reaction rate (via modifying the magnitude of K_{chem}) one observes shift of the first electron transfer step towards more positive potentials. Such scenario in Figure 8 occurs for $K_{chem} > 0.1$ (Figure 8d), and for magnitudes of chemical equilibrium constant $K_{eq} > 0.5$. For $K_{chem} > 0.2$ (Figure 8e-f), two well-separated processes are observed: one peak that exists at a potential of 0.0 V, while the second peak that appears at about +0.140 V. Once both SW peaks are separated for at least 150 mV (Figure 8d-e), then one can apply a suitable methodology to get access to the relevant kinetic parameters of all steps involved in this complex mechanism, following the procedures elaborated in [7,16-18].

If both electron transfer steps of a given surface $EC_{rev}E$ mechanism are very fast, then a net-SW peak splitting phenomenon appears [7,8,24]. If both electron transfers take place at the same potential, a single split net SW peak features both electron transfer steps (Figure 9a). In such scenario, one can also achieve a separation between the two-electron transfers of surface $EC_{rev}E$ mechanism via modifying the magnitude of K_{chem}. An example is represented in patterns of Figure 9b-f. At defined magnitudes of K_{chem}, one observes voltammograms consisting of one "split SW net peak" that is related to the second electron transfer step (peak II, positioned at more negative potentials), and a single net peak (peak I) displaced to more positive potentials (figure 9e-f). The last is related to the first electron transfer step, whose position is altered to more positive potentials under the influence of increased rate of chemical step.

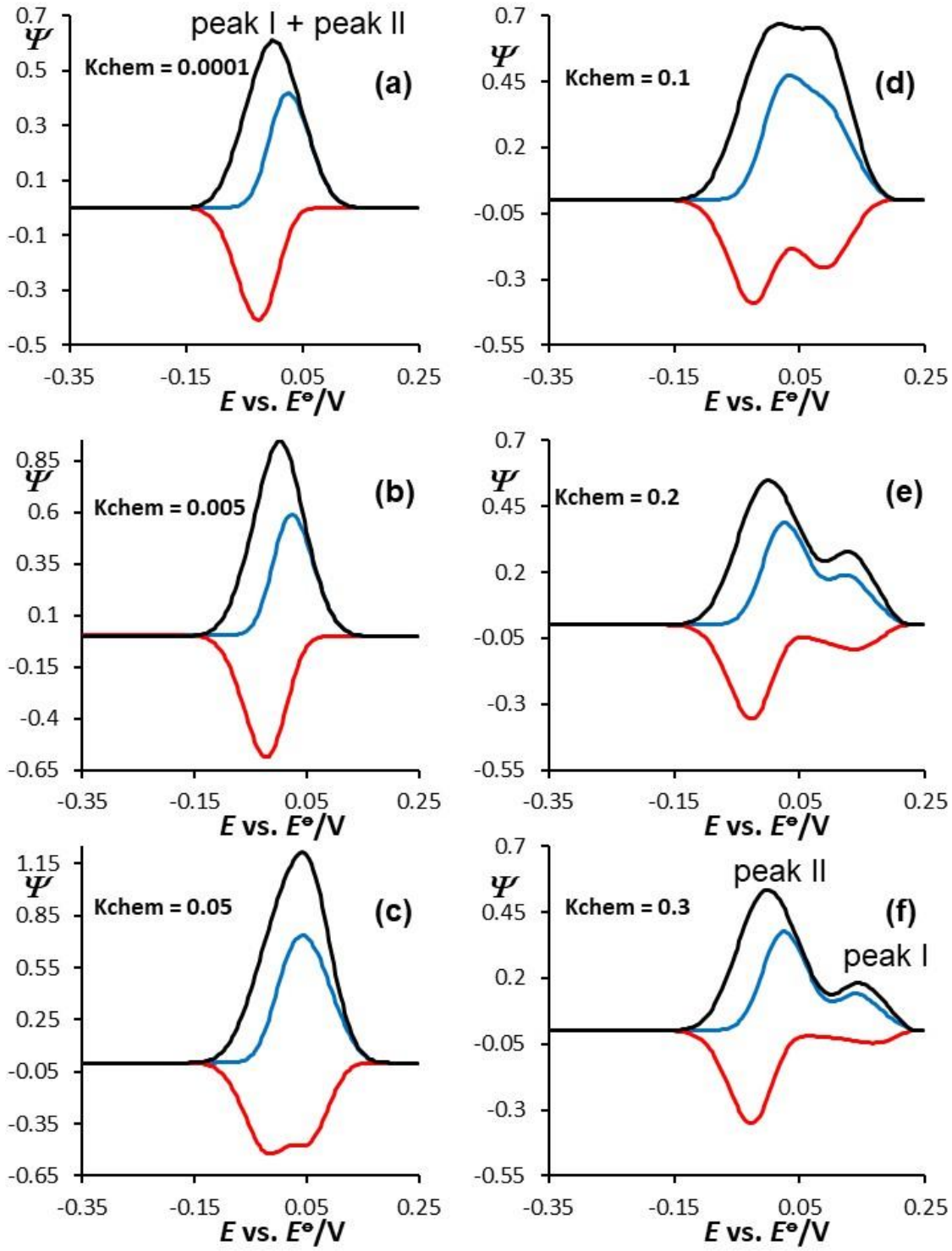

Figure 8. Theoretical SW voltammograms of a surface $EC_{rev}E$ mechanism representing the effect of the dimensionless rate parameter of the chemical step K_{chem} in scenario of both electron transfer steps happening at same potential. The magnitude of chemical equilibrium constant was set to $\boldsymbol{K_{eq} = 10}$. The values of both *K*I and *K*II were set to 2.0. The magnitudes of K_{chem} used in simulations are given in the charts. Other simulation parameters were same as those in Figure 1.

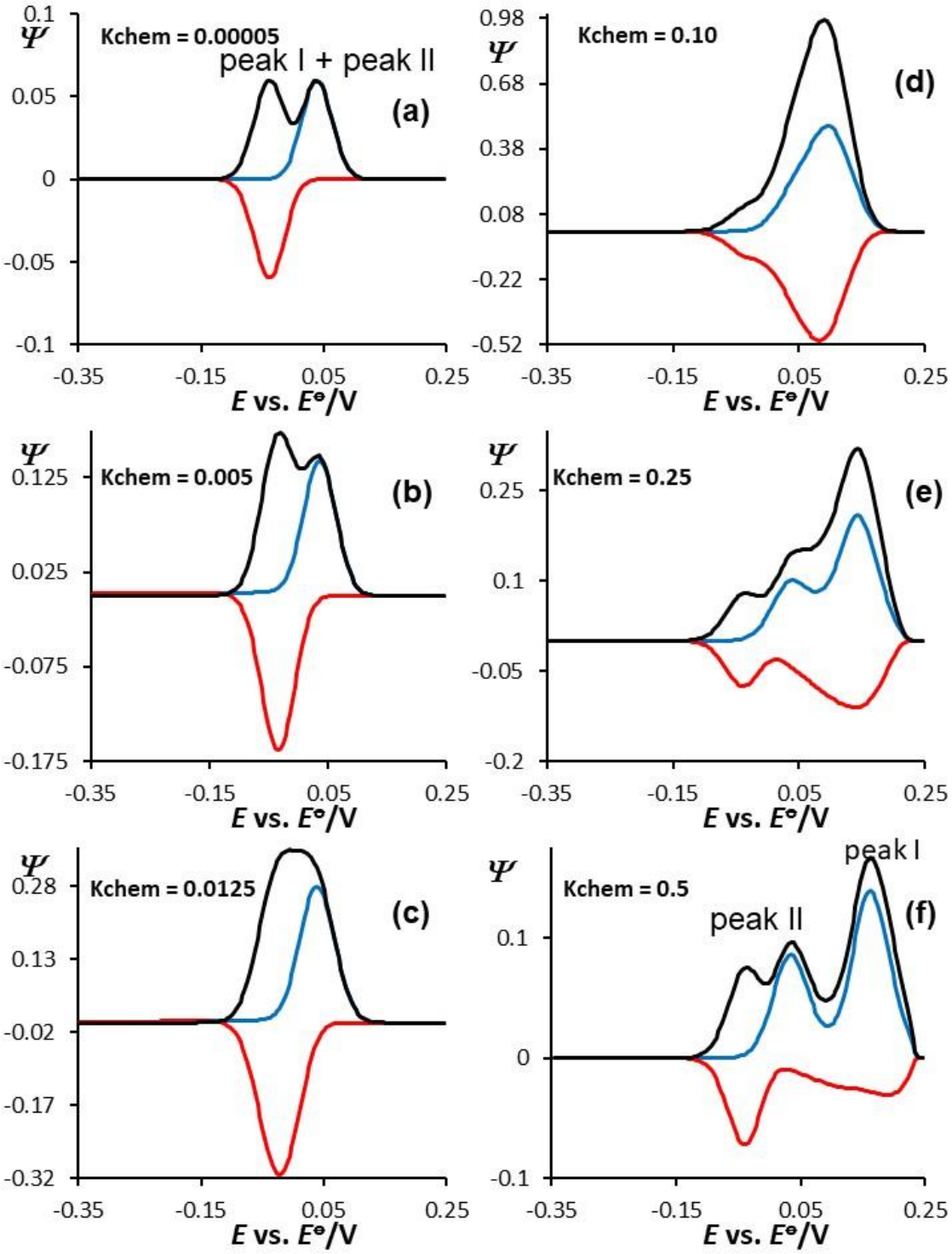

Figure 9. Theoretical SW voltammograms of a surface EC$_{rev}$E mechanism showing the effect of the dimensionless rate parameter of the chemical step K_{chem} in the scenario of both electron transfer steps happening at the same potential. The magnitude of the chemical equilibrium constant was set to $\boldsymbol{K_{eq} = 100}$. The magnitudes of both *K*I and *K*II were set to 5.0 (region of fast electron transfer). The magnitudes of K_{chem} used in simulations are given in the charts. Other simulation parameters were the same as those in Figure 1.

Once separation of about |150 mV| or more between both peaks is achieved (Figure 9e-f), then one can apply suitable methodologies to get access to all relevant kinetic and thermodynamic parameters relevant to all steps involved in this mechanism [7,16-18]. From the voltammetric patterns elaborated in Figures 8 and 9, one gets enough information on how to separate two overlapped electron transfer steps of a surface $EC_{rev}E$ mechanism via modifying the kinetics of the chemical reaction coupled to the electron transfer steps. Indeed, this is a very useful methodology that can be applied experimentally to characterize many systems with inverted redox potentials.

4. CONCLUSIONS

Although several models of ECE mechanisms taking place from dissolved state are already considered under voltammetric conditions [6, 25-30], in this work we consider for the first time an $EC_{rev}E$ mechanism, with all electroactive species being strongly adsorbed at the working electrode surface. The model is suitable to analyse the redox chemistry of many important lipophilic physiological systems such as lipophilic quinones and polyphenols, cytochromes and many lipophilic redox enzymes. In the majority of the mentioned systems, it is almost inevitable to have a chemical reaction (mainly protonation/deprotonation) that is associated to both electron transfers under physiological conditions. If both electron transfer steps of a surface $EC_{rev}E$ mechanism take place at potentials that are at least -150 mV separated from each other, then the electrochemistry of such systems will be portrayed in voltammetric patterns featuring two well-separated SWV peaks. Under defined conditions, the first peak (at more positive potentials) has attributes typical of a surface EC_{rev} mechanism, while the second peak (positioned at more negative potentials) gets features of a surface $C_{rev}E$ mechanism. However, in case of both electron transfers having "inverted redox potentials", a single square-wave voltammogram will be obtained (figures 5 and 6) that "hides" in its shape the features of both electron transfer steps and those of the chemical reaction. Successful separation of both "overlapped" electron transfer steps can be achieved via modifying the chemical kinetic parameter K_{chem}. An increase of K_{chem} (for systems with $K_{eq} > 0.5$) leads to displacement of the first electron transfer step towards more positive potentials. Eventually, separation of both electron transfers is achieved at higher rates of the chemical reaction. This, in addition, enables the application of a suitable methodology for kinetic and thermodynamic characterization of both electron transfer steps, and the chemical step as well, as reported elsewhere [7,16-18]. Since K_{chem} is defined as $K_{chem} = [k_f^{\theta'} c(Y) + k_b]/f$, one recognizes that modification of K_{chem} can be achieved via altering the SW frequency f, or by modifying the concentration of substrate Y. As the SW frequency has a simultaneous effect on the kinetics of electron transfers of both steps, and to the value of dimensionless rate parameter K_{chem} as well, time analysis is not recommended to be applied in such scenario in SWV. Thus, in order to obtain separation of both electron transfers with inverted potentials in SWV, we advise experimentalists to modify

the rate of chemical reaction by altering the concentration of *c*(Y), while performing experiments at constant SW frequency. For getting access to the kinetics and thermodynamics of chemical step of a surface $EC_{rev}E$ mechanism, one can take advantage of the methodologies reported in [7,16-18].

Acknowledgments

Rubin Gulaboski thanks the Alexander von Humboldt Foundation for the support in 2021 for the research stay at the University of Goettingen, Germany.

REFERENCES

[1] L. Meites, P. Zuman, and A. Narayanan, CRC Handbook Series in Inorganic Electrochemistry; CRC Press, Vols. 1-8 (1980-1988).

[2] P. N. Barlett, Bioelectrochemistry: Fundamentals, experimental techniques, and application, Wiley, Chichester, UK (2008).

[3] A. J. Bard (Ed.) Encyclopedia of electrochemistry; Marcel Dekker, New York, Vols. 11-15 (1978-1984).

[4] H. Sies, and L. Parker Quinones and quinone enzymes; in Methods in enzymology, Academic Press, UK (2004).

[5] F. A. Armstrong, Electrifying metalloenzymes in: Metalloproteins: Theory, calculations and experiments (Cho AE, Goddar III WA, eds), CRC Press, Taylor & Francis Group, London, New York USA (2015).

[6] R. G. Compton, and C. E. Banks, Understanding voltammetry, 2nd Edition, Imperial College Press, London, UK (2011).

[7] V. Mirceski, S. Komorsky-Lovric, and Lovric, Square-wave voltammetry, Theory and application, (Scholz, F. ed.), Springer, Berlin, Germany (2007).

[8] M. Janeva, P. Kokoskarova, V. Maksimova, and R. Gulaboski, Electroanalysis 31 (2019) 2488.

[9] R. Gulaboski, V. Mirceski, I. Bogeski, and M. Hoth, J. Solid State Electrochem. 16 (2012) 2315.

[10] R. Gulaboski, J. Solid State Electrochem. 13 (2009) 1015.

[11] C. Leger, S. J. Elliott, K. R. Hoke, L. J. C. Jeuken, A. K. Jones, and F. A. Armstrong Biochem. 42 (2003) 8653.

[12] L. P. Jenner, and J. N. Butt, Curr. Opin. Eletrochem. 8 (2018) 81.

[13] F. A. Armstrong, H. A. Heering, and J. Hirst, Chem. Soc. Rev. 26 (1997) 169.

[14] F. A. Armstrong, Voltammetry of proteins. in: Encyclopaedia of electrochemistry (A. J. Bard, M. Stratmann, and G. S. Wilson, eds), Wiley VCH, Weinheim (2002).

[15] R. Gulaboski, V. Mirceski, and M. Lovric, Maced. J. Chem. Chem. Eng. 40 (2021) 1.

[16] R. Gulaboski, M. Janeva, and V. Maksimova, Electroanalysis 31 (2019) 946.
[17] R. Gulaboski, V. Mirceski, and M. Lovric, J. Solid State Electrochem. 23 (2019) 2493.
[18] R. Gulaboski, V. Mirceski, M. Lovric, and I. Bogeski, Electrochem. Commun. 7 (2005) 515.
[19] R. Gulaboski, Electroanalysis 31(2019) 545.
[20] V. Mirceski, E. Laborda, D. Guziejewski, and R. G. Compton, Anal. Chem. 85 (2013) 5586.
[21] D. H. Evans, and K. Hu, J. Chem. Soc. Farad. Trans. 92 (1996) 3983.
[22] N. A. Ruvalcaba, and D. H. Evans, J. Phys. Chem. B 110 (2006) 5155.
[23] R. Gulaboski, I. Bogeski, P. Kokoskarova, H. H. Haeri, S. Mitrev, M. Stefova, J. Stanoeva Petreska J, V. Markovski, V. Mirceski, M. Hoth, and R. Kappl, Bioelectrochem. 111 (2016) 100.
[24] V. Mirceski, and M. Lovric, Electroanalysis 9 (1997) 1283.
[25] J. J. O'Dea, K. Wikie, and J. Osteryoung, J. Phys. Chem. 94 (1990) 3628.
[26] A. Molina, M. Lopez-Tenez, C. Sern, M. M. Moreno, and M. Rueda, Electrochem. Commun. 7 (2005) 751.
[27] A. Molina, E. Laborda, J. M. Gomez-Gil, F. Martinez-Ortiz, and R. G. Compton, Electrochim. Acta 195 (2006) 230.
[28] A. M. Mann, J. C. Helfrick, and L. A. Bottomley J. Electrochem. Soc. 163 (2015) H3101
[29] S. Komorsky-Lovric, and M. Lovric, Anal. Bioanal. Electrochem. 5 (2013) 291.
[30] A. R. Dale-Evans, M. J. Robinson, H. O. Lloyd-Laney, D. J. Gavaghan, A. M. Bond, and A. Parkin, Front. Chem. (2021) doi.org/10.3389/fchem.2021.672831.